

Study of the Effect of Magnetic Serum Albumin Nanoparticles on Cultured Mice Renal Mesangial Cells and Submandibular Cells Using Different Biological Assays

Naif Al Qurashi

Department of Basic Science, Deanship of Preparatory Year and Supporting Studies, Imam Abdulrahman Bin Faisal University, Dammam, SAUDI ARABIA.

ABSTRACT

Background: Bovine Albumin Nanoparticles (BAN) have a high magnetic susceptibility and great potential for biomedical applications. **Aim:** Evaluate the *in vitro* effects of magnetic BAN on mouse renal and submandibular cells. **Materials and Methods:** The ferromagnetic iron oxide Nanoparticles (NPs) were lyophilized and diluted in Dulbecco's modified eagle culture medium. The diameters of the NPs were measured. Mouse renal and submandibular cells were cultured from an initial passage of 3×10^6 cells in 100 cm² culture flasks. Bovine Albumin Nanoparticles were applied to the culture at a concentration of 260, 160 and 85 µg/mL to test the number of viable or degenerating cells. Detection of apoptic and necrotic cells were carried out using the color variability and the nucleus morphology, chromatin condensation and fragmentation. **Results:** The staining test with acridine orange and ethidium bromide allowed the distinction between viable, necrotic and apoptotic cells in each of the experimental groups. Frequency of cells in degeneration was significantly greater in the BAN-treated groups at concentration 260 µg/mL and 160 µg/mL. The comet assay revealed the frequency of cells with DNA damage; Mouse renal cells have an irregular shape, a large nucleus and numerous cytoplasmic projections. Their cytoplasm is rich in membranous organelles, maintaining the characteristic ultrastructure pattern of secretory cells. Mouse submandibular cells treated with BAN showed no changes in ultrastructure but had agglomerates of NPs inside and a greater amount of BAN agglomerates in the outside. **Conclusion:** Results obtained in this article point to the biocompatibility of the sample of magnetic albumin polymers.

Keywords: Bovine albumin nanoparticles, Mouse renal and submandibular cells, Genotoxicity, Cytotoxicity, Degenerative cells.

Correspondence:

Associate Professor. Naif Al Qurash

Department of Basic Science, Deanship of Preparatory Year and Supporting Studies, Imam Abdulrahman Bin Faisal University, P.O. Box 1982, Dammam, SAUDI ARABIA.
Email: nalqurashi@iau.edu.sa
ORCID ID: 00 00000344883506

Received: 30-03-2023;

Revised: 14-01-2024;

Accepted: 13-05-2024.

INTRODUCTION

Nanoparticles (NPs) exhibit significantly different physical, chemical and/or biological properties. They are applied successfully in the field of nanotechnology. Their diameter measures 1-100 nm.^{1,2} Nanostructured materials have stood out in the biomedical areas for presenting features such as a high surface/volume ratio and the capacity for responding to a magnetic field gradient. Furthermore, when NPs are scaled to nanometer, they behave like super-paramagnetic particles, or they do not retain magnetism after removal of the magnetic field.³ Among the several biomedical applications of Nanoparticles (NPs): the separation, diagnostic imaging of magnetic resonance, the purification and concentration

of biomolecules and cells, induction of hyperthermia for the treatment of several pathologies, in particular cancer and site-specific drug delivery system.⁴ To separate, purify and concentrate biomolecules and cells, NPs are usually associated with molecules which can identify them. When they are added to a solution, or suspension, containing these biomolecules or/and cells, NPs form a complex which can be collected by means of a magnetic separator.⁵ A case of particular cell sorting can be achieved by linking NPs to a specific antibody. When target cells are recognized by the antibody, they are magnetically marked and, in this way, they are separated by means of magnetic columns and removed with the aid of an external magnet.⁶ Using this immune-magnetic separation technology, Yildiz, 2016 and Alvieri, *et al.* 2020.^{7,8} were able to isolate the human protein CD¹⁴⁺ from neutrophils and dendritic cells. Papadimitriou, *et al.* 1995⁹ succeeded to isolate the hematopoietic stem cell CD³⁴⁺ from human peripheral blood for cell transplantation therapies. NPs, even at low concentrations, are captured by cells and remains there for the time necessary for diagnosis. The effectiveness of



DOI: 10.5530/ijper.58.3s.83

Copyright Information :

Copyright Author (s) 2024 Distributed under Creative Commons CC-BY 4.0

Publishing Partner : EManuscript Tech. [www.emanuscript.in]

NPs depends on their physicochemical properties such as size and connection they establish with other molecules, such as those used to coat them, which affect their pharmacokinetics and bio-distribution.¹⁰ Liver-specific NPs were used as contrast agent for the first time in 1995.¹¹ Since then, several works have shown that NPs, mainly those of iron oxide, are transmitted spontaneously and preferably to lymph nodes. By means of magnetic resonance imaging, metastases of lymph nodes and testicular tumors can be detected at an early stage,¹² bladder, prostate, urethra, breast, colon¹³ and stomach.¹⁴ NPs can be used as drug delivery systems in specific sites, such as for the treatment of several diseases, including cancer. So, the NPs associated with chemotherapy drugs can be taken to a specific location through an external magnetic field, increasing the effectiveness of the treatment and reducing side effects in normal tissues.¹⁵ These authors used iron oxide NPs associated with the chemotherapy drug 4-epidoxorubicin with trade name pharmorubicin[®] in patients with axillary node metastases and demonstrated that the nanoparticle-chemotherapeutic complex was not toxic and accumulated in tumor tissue. More recently, Heidari, *et al.* 2013¹⁶ administered NPs conjugated to the chemotherapy drug mitozantrone in rabbits and observed that this complex appeared more concentrated in the tumor tissue, even when only minimal percentage of the free chemotherapy dose was applied. In addition to the aforementioned applications, NPs can be used to destroy tumor cells (magnetic thermocytolysis), because when they are submitted to a field they alternate the frequency magnets, absorb energy which is converted into heat and induce hyperthermia. In magnetically hyperthermia generated, the temperature in tumor cells can reach up to 42°-45°C,¹⁷ enough heat to destroy them. Heat is normally dissipated by blood circulation, but tumor tissues have a disordered network of blood vessels, which make the blood circulation slow and irregular, making the cells more susceptible to heat. Several studies show that hyperthermia induces damage to the cytoskeleton, to the plasma membrane and the membranes of organelles, such as those of mitochondria, lysosomes and endoplasmic reticulum. In addition, it increases the immunogenicity of the tumor, potentiates the effects of radiotherapy and enhances the action of antineoplastic drugs.¹⁸ The role on the effects of radiotherapy and antineoplastic drugs is probably due to increased tissue perfusion, induction of dispersion of oxygen radicals in the radiotherapy and more appropriate distribution of antineoplastic drugs.¹⁹ Considered non-toxic, the most tested NPs in biomedical applications are those of iron oxide, whether in the form of magnetite (Fe₃O₄) or in its oxidized form, the maghemite (Fe₂O₃, γ-Fe₂O₃).

In order to carry out biomedical applications of NPs, researchers developed an ionic magnetic fluid consisting of maghemite NPs that, subsequently, they were encapsulated in Bovine Albumin Nanoparticles (BAN) which showed a high magnetic susceptibility. Due to this feature, this new material should enable magnetic hyperthermia, as well as favor the delivery of site-specific drugs.

Prior to their use in biomedical applications, however, effects of administering new materials must be tested in biological systems. Among the models of *in vitro* experiments, different cell lines can be used, including Mouse Submandibular Salivary Gland (MSG) and Mouse Renal Mesangial Cells (MRMC). Cell lines have assumed an important role in studying physiological, pathophysiological, and differentiation processes of specific cells. The extreme difficulties in the isolation and purification of individual epithelial cells from complex tissues by maintaining their native characteristics have hampered our understanding of their physiological, biological, growth, and differentiation characteristics. As in the case of irradiated human salivary gland,²⁰ the MRMC line has been used in cytotoxicity and genotoxicity tests of therapeutic substances²¹ and in cell differentiation studies.²² In turn, the submandibular gland ductal cell line was immortalized from a culture of primary cells.²³ It is one of the cell types found in the glomeruli of the kidneys, in the intercapillary spaces immersed in a mesangial matrix. They participate, by contraction, in intraglomerular hemodynamics, and the rhythm of glomerular filtration, in addition to having phagocytic and clearance of substances such as immunocomplexes. Mesangial cells have been used in cytokine cytotoxicity tests.²⁴

This article aims to evaluate the *in vitro* effects of magnetic BAN. Determine the modal diameter of the NPs constituents of magnetic BAN; Evaluate possible cytotoxic effect of different concentrations of magnetic albumin polymers in MRMC and MSG by means of acridine orange ethidium bromide assay; Determine the main route of cell degeneration after treatment with magnetic BAN; Evaluate the possible genotoxic effect of magnetic BAN in MRMC and MSG through the comet assay; Verify a possible relationship between cytotoxicity and genotoxicity of magnetic BAN and investigate the occurrence of morphological and ultrastructure alterations and interiorization of NPs in magnetic BAN -treated MRMC and MSG.

MATERIALS AND METHODS

Magnetic Albumin Polymers²⁵

The ferromagnetic iron oxide, Maghemite (Fe₂O₃, γ-Fe₂O₃) NPs from a magnetic fluid sample of ionic acid (2.17×10²⁸ particles/mL) were dispersed in an aqueous albumin solution and subsequently lyophilized, with a final concentration of 2.51×10²⁶ particles/mg. The ionic magnetic fluid was synthesized and its NPs were encapsulated in BAN. For cell treatment, magnetic BAN were diluted in Dulbecco's modified eagle culture medium (Thermo Fisher Scientific[®]-US), in order to obtain different concentrations. To determine the diameter of NPs of the albumin polymers, samples were solubilized in Phosphate buffer saline pH 2.5 to increase dispersion and facilitate counting. By co-precipitating Fe(II) and Fe(III) chlorides by ammonium hydroxide and then oxidizing, respectively, and thermally breaking down Fe(III) carboxylates in the presence of oleic acid, iron oxide nanoparticles

with uniform sizes ranging from 5 and 150nm and polydisperse 14 nm were produced. The second procedure created hydrophilic, but uncoated, nanoparticles, whereas the first method produced hydrophobic, oleic acid-coated particles. The surface of the iron oxide particles was treated with poly (ethylene glycol) and sucrose, respectively, to make them colloiddally stable and water soluble. X-ray diffraction, dynamic light scattering, and transmission electron microscopy were used to determine the size and size distribution of the nanoparticles. The surfaces of the iron oxide particles treated with sucrose and functionalized with PEG were examined using Fourier Transform Infrared (FT-IR) and Raman spectroscopy. NPs were analyzed and photographed. The diameters of the NPs ($n=400$) were measured using electron microscopy coupled to spectroscopic methods to perform elemental analysis. The particle distribution was achieved using the best lognormal fit.

Maintenance and propagation of MRMC and MSG²⁶

MRMC and MSG were added to fetal bovine serum 10%, streptomycin-penicillin 1.2%, buffered with sodium bicarbonate, with pH 7.6 adjusted by addition of hydrochloric acid. Cultures were established from an initial passage of 3×10^6 cells in 100 cm² culture flasks and kept in an oven at 37°C, in an atmosphere 4% CO₂ and saturated humidity. Once 85-95% of confluence is reached, the cells were released from the bottom of the culture flask by treatment with trypsin solution and 0.110%/EDTA 0.02% for 2 min, centrifuged at 180g for 5 min, counted in a counting chamber BLAUBRAND[®] Neubauer (Sigma-Aldrich) and transferred to a new culture flask.

Determination of BAN concentrations to be administered to MRMC and MSG²⁷

In order to determine the concentration of magnetic BAN administered to the cells to carry out the biological assays, cell viability tests were carried out in triplicate. The cultures were maintained in 9-well plates initially containing 2×10^6 cells. The initial concentrations of BAN were defined from the concentrations previously tested,³⁰ in melanocyte culture. After 24 hr of cultivation in BAN samples, cells were trypsinized, centrifuged and resuspended in 2.2 mL of culture media.

Treatment of MRMC and MSG with BAN²⁸

Based on the BAN concentrations used in the viability tests and their results, the concentrations added to the cultures were established, kept for 24 hr biological assays were performed. So, follow the standards established in the studies of genotoxicity and cytotoxicity, it included the positive control, consisting of a group of cells treated for one hour with hydrogen peroxide at a final concentration of 1 mM (20 µg/mL).

Distinguishing between apoptosis and necrosis degeneration pathways by means of staining with acridine orange and ethidium bromide²⁹

For the Acridine Orange (AA) and Ethidium Bromide Staining Assay (BE), performed in triplicate, MRMC and MSG were cultivated and maintained. After 24 hr of passing the cells, each experimental group received the respective treatment, after 24 hr of treatment, the cells in suspension and those adhered to the flasks were collected, subjected to centrifugation at 740g for 5 min and resuspended in 100 µL of culture medium. From each sample, 20 µL were removed and subsequently added 2 µL of a freshly prepared mixture of the acridine orange (100 µL/mL water) and ethidium bromide (100 µL/mL water), in the 1:1 ratio. The stained cells were then immediately placed on glass slides (25×70 mm), previously washed and identified and, after assembly with coverslips (24×24 mm) were analyzed by means of a blind test, under a light microscope. Fluorescence (Olympus, 530 nm dam filter) used for photography. About 300 cells were analyzed from each treatment, 100 cells in each of the triplicates, as a minimum.

Criteria for classifying cells as apoptotic, necrotic or viable³⁰

Analyzes for detection of apoptic and necrotic cells quantification were carried out using the variability in color and the nucleus morphology, the chromatin fragmentation and condensation. This differentiation is attainable because, while the Acridine orange (AA) penetrates dead and living cells, generating green fluorescence emission by intercalating in DNA and orange in RNA, Ethidium Bromide (EB) only passes through cells that already have changes in the membrane (late apoptic or necrotic), emitting an orange fluorescence when intercalating in the DNA.

Evaluation of DNA damage of isolated cells in microgel Comet Assay³¹

The comet assay was carried out in triplicate. For this test, MRMC and MSG were cultured and maintained. After 24 hr of cultivation, each experimental group received the respective treatment. After 24 hr of treatment, the culture medium was removed and placed in centrifuge flasks to which the cells were added after being released from the board background. The samples were then centrifuged at 740 g for 5 min and the resuspended cells in 1 mL of PBS. This procedure was repeated for two times. Cells were resuspended in 20 µL of low melting point agarose (Low melting point - LPM-Sigma, USA) at 0.5% in PBS and heated to 37 °C in a water bath. Immediately after this procedure, 130 µL of this mixture were dropped into a 26 × 76 mm glass slide, previously prepared. The preparation of the slides was carried out immersing them in type II agarose diluted in 1.5% PBS and then keeping them at room temperature for a period of 12 hr. After dripping the cells into LPM agarose on the slides, a coverslip was attached to each slide and the set was placed in the refrigerator.

Criteria for DNA damage analysis³²

DNA damage was assessed using a light microscope. fluorescence, Axioplan imaging* (Carl Zeiss AG, Germany) using 510-560 nm filter, 590 nm filter barrier and total magnification of 400×. From each treatment, about 300 nucleotides, 100 in each of the triplicates, in the minimum, were analyzed in a blind test and classified according to the length of the tail of the nucleoid, in which the analyzed nucleoids are classified from 0 to 4, according to their degree of injury. For quantification of DNA damage, the total score for the 300 nucleotides analyzed ranges from 0 (minimum damage = no cells damaged) to 400 (maximum damage=all nucleoids with class 4 damage), being estimated from the formula: $ID (AU) = \frac{N1 + 2N2 + 3N3 + 4N4}{n} / 100$; Where, ID=DNA damage index; AU arbitrary unit; N1...N 4=nucleoids classified as class 1, 2, 3 or 4; n=number of nucleotides analyzed, including class zero.

Statistical Analysis

For statistical analysis of DNA damage rates found in cells MRMC, Analysis of Variance (ANOVA) was applied. In cases where they were detected differences between treatments, the Fisher test was applied at a significance level of 5% ($p < 0.05$). In the MSG, the “box cox” transformation was used; suitable for absolute numbers and then Analysis of Variance (ANOVA) was applied. Of same way as used for MRMC when they were detected differences between treatments in MSG, the Fisher test was applied at the level of significance 5% ($p < 0.05$). For statistical analysis of the frequency of cells with DNA damage checked in MRMC, Analysis of Variance (ANOVA) was also applied and, when differences between treatments were detected, the Fisher test was applied at the level of significance 5% ($p < 0.05$).

Processing of MRMC and MSG for analysis of cell morphology in light microscopy

Cells were prepared for morphological analysis in a culture plate of six wells, containing a microscopy coverslip (18×18 mm) in each well. 2×10⁵ cells were initially cultured and grown adhered to the coverslips. After 24 hr, each experimental group received treatment with the BAN sample (260 µg/mL, 160 µg/mL and 85 µg/mL). Tests were performed in duplicate. After the time of treatment, the culture medium was removed and the cells washed three times with PBS (NaCl 0.154 M; 0.1M Na₂HPO₄; pH 7.4). Cells adhered to one of the coverslips were fixed with 2% paraformaldehyde in phosphate buffer for 10 min. After being washed with PBS, the cells were stained with a solution of 0.2% cresyl violet in 20% ethanol for 5 min. The cells adhered to the other coverslip, in each of the experimental groups, were stained with 4% Giemsa solution in methanol, for 5 min, without going through a fixation.

Processing of MRMC and MSG for analysis of cell morphology in Transmission electronic microscopy

For the analysis of the ultrastructure, cell cultures were maintained. After the adhesion of the cells to the bottom of the flask, the BAN sample was added to the culture. After 48 hr of treatment, the culture medium was removed and placed in centrifuge flasks to which the cells were added previously trypsinized. The samples were then centrifuged at 740 g for 5 min, and the cells resuspended in 1 mL of PBS. This procedure was repeated twice times. The cells, after being trypsinized and centrifuged.³² The cells were resuspended in 1 mL of fixative consisting of 2% glutaraldehyde, 4% paraformaldehyde, diluted in 0.1 M sodium cacodylate buffer, pH 7.4, and 2% sucrose. After one hour, the samples were centrifuged at 740g and washed, for 10 min, with sodium cacodylate buffer (0.1 M, pH 7.4) plus sucrose 4%. This procedure was repeated twice. Then, the samples were post-fixed for one hour, protected from light, in a mixture composed of 1% osmium tetroxide, 0.8% potassium ferricyanide and 5mM calcium chloride diluted in sodium buffer (0.1 M, pH 7.4). After being washed twice with sodium cacodylate buffer for 10 min, cells were stained in block with 0.5% aqueous uranyl acetate for one hour, protected from light. They were then washed with sodium cacodylate buffer, for 10 min and then with distilled water. The cells were then dehydrated in increasing concentrations of acetone: 30%, 50%, 70%, 90% and 100% (this last repeated three times). Dehydration time was 10 min for each of acetone concentrations.

RESULTS

Animal cell culture is now essential for scientific, biotechnological, and diagnostic research. Alongside this advancement, biosafety concerns have also emerged, drawing attention to the possible risks handling animal cell cultures poses to human health and, to a lesser extent, the environment. To control these risks, a thorough risk assessment of the cell cultures and the type of manipulation is required before starting any activity. It involves evaluating each case separately for cell cultures that have been genetically engineered or not, as well as the possibility that they could purposefully or inadvertently come into contact with hazardous microbes. The latter risk is more likely to materialize when adventitious contaminants are pathogenic or have a higher capacity to endure in harsh conditions.

Magnetic Albumin Polymers

Results of the biological effects of magnetic NPs contained in bovine albumin polymers using different biological assays are described in Figures 1 to 5. One of the experimental approaches initially carried out was the determination of the diameter of the maghemite particles present in the BAN samples, which was performed through Transmission Electron Microscope (TEM) analysis. At the BAN, the NPs were slightly spherical (Figure 1a).

Table 1: Different concentrations of BAN showed different viabilities of MRMC and MSG cell lines.

Concentration of BAN	Survival of MRMC	Survival of MSG
120 µg/mL	65%	70%
260 µg/mL	60%	65%
160 µg/mL	61.5%	60%
85 µg/mL	32.5%	55%

The analysis of 400 particles in the photomicrographs showed diameters ranging between 5 and 150 nm, which demonstrates that these particles are, Mult dispersed (Figure 1b).

Maintenance and propagation of MRMC and MSG

To determine the concentration of magnetic albumin polymers (BAN) to be administered to the cells of the genotoxicity tests, viability tests with MRMC and MSG cell lines. As shown in Figure 1c and Table 1, magnetic albumin polymers at different concentrations showed different viabilities.

Determination of BAN concentrations to be administered to MRMC and MSG

Because albumin nanoparticles may be made in soft circumstances and include a variety of compounds, they are an appealing drug delivery strategy. The purpose of this work was to use a membrane contactor to advance the desolvation process for the creation of Bovine Albumin Nanoparticles (BAN). First, a syringe pump was used to create the BAN nanoparticles on a small scale. Using the following ideal parameters, with uniform sizes ranging from 5 and 150nm BAN nanoparticles with a polydispersity index of 0.047 were produced: pH 8.1, 100 mg mL⁻¹ BAN albumin solution (4 mL), and 2 mL min⁻¹ flow rate of oleic acid-coated particles (8 mL).

Treatment of MRMC and MSG with BAN

The staining test with acridine orange and ethidium bromide allowed the distinction between viable, necrotic and apoptotic cells in each of the experimental groups. Figure 1e and Table 2 illustrate the frequency of MRMC cells in the process of degeneration, as well as its path of degeneration. It can be seen that the frequency of cells in degeneration was significantly greater in the BAN-treated groups at different concentrations. The route of most frequent degeneration was apoptosis. This is only smaller than the necrosis in the control positive. MSG cells were also evaluated for cell degeneration and the results are illustrated in Figure 1f. Unlike what happened in MRMC, in MSG only at a concentration of 260 µg/mL BAN induced a considerable frequency of cells in degeneration as shown in Table 3.

Distinguishing between apoptosis, necrosis and degeneration pathways by means of staining with acridine orange and ethidium bromide and Evaluation of DNA damage of isolated cells in microgel Comet Assay

As in MRMC, in MSG the most common degeneration pathway frequent, both in the groups treated with BAN and in the untreated one, were apoptosis, except for the positive control (Figure 1f). In the comet assay, for each cell lineage, about 250 nucleoids per treatment were tested. The different classes of comet were detected in almost all experimental groups. The results obtained for each cell line are presented in two ways: Frequency of cells with DNA damage, which indicates the frequency of cells in each experimental group, classified as class 1, 2, 3 and 4 comets; and index of DNA damage, which reflects the intensity of DNA damage in cells.

Criteria for classifying cells as apoptotic, necrotic or viable

The frequency of MRMC cells with DNA damage is shown in Figure 1g and Table 4. The frequency of MSG with DNA damage is shown in (Figure 1h).

Criteria for DNA damage analysis and Processing of MRMC and MSG for analysis of cell morphology in light microscopy

Regarding the index of DNA damage presented by the MSG (Figure 1i and 1j), data analysis showed that the index of the groups treated with BAN (260 µg/mL, 160 µg/mL and 85 µg/mL -95, 99 and 91, respectively) is significantly higher than that of the control group (2.22 AU). In order to verify whether BAN induced changes in the morphology and ultrastructure of the cells, they were analyzed under a light microscope and an electron microscope of transmission. Under the light microscope, untreated MRMC are polygonal shaped which can vary from little elongated to more rounded according to the confluence of culture and cytoplasmic projections which connect one cell to another. The nucleus of these cells is spherical or ovoid, with one or two nucleoli evident. Treatment with BAN, at different concentrations, did not induce changes in the morphology of these cells. Treatment with BAN, at different concentrations, did not induce changes in the morphology of these cells, as illustrated in Figure 2 (c and d). MSG are irregularly shaped, have long cytoplasmic processes which give a starry appearance. They have an oval, central nucleus with evident nucleoli (Figures 3a and 3b). When treated with BAN sample, the MSG did not show morphological changes (Figure 3c). However, clusters of magnetic albumin polymers, apparently not internalized by cells (Figure 3d).

Table 3: Shows the frequency of MSG cells in degeneration was significantly greater in the BAN-treated groups at different concentrations.

BAN concentrations	Degenerative MSG cells
Negative control	12.7%
260 µg/mL	25.7%
160 µg/mL	17.2%
85 µg/mL	12%

Table 2: Shows the frequency of MRMC cells in degeneration was significantly greater in the BAN-treated groups at different concentrations.

BAN concentrations	Degenerative MRMC cells
Negative control	7.22%
260 µg/mL	18.55%
160 µg/mL	13.65%
85 µg/mL	12%

Table 4: Shows the frequency of MRMC cells with DNA damage.

BAN concentrations	Frequency of cells with DNA damage	Damage index
Negative control	8%	4.22 AU
260 µg/mL	85.22%	130 AU
160 µg/mL	55.44%	59 AU
85 µg/mL	37.23%	44 AU

Processing of MRMC and MSG for analysis of cell morphology in Transmission electronic microscopy

To elucidate the effects of BAN on the ultrastructure of cells and to investigate a possible internalization of magnetic NPs a study was carried out by TEM. At TEM, MRMC have an irregular shape, a large nucleus and numerous cytoplasmic projections. Their cytoplasm is rich in membranous organelles, maintaining the characteristic ultrastructure pattern of secretory cells. When treated with BAN, these cells showed no changes. However, despite the light microscope, they are not visualized BAN NPs

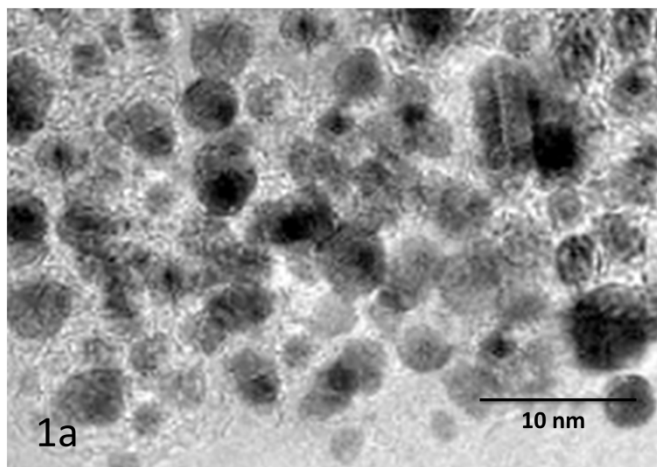


Figure 1a: TEM showing the diameter of the maghemite Albumin particles.

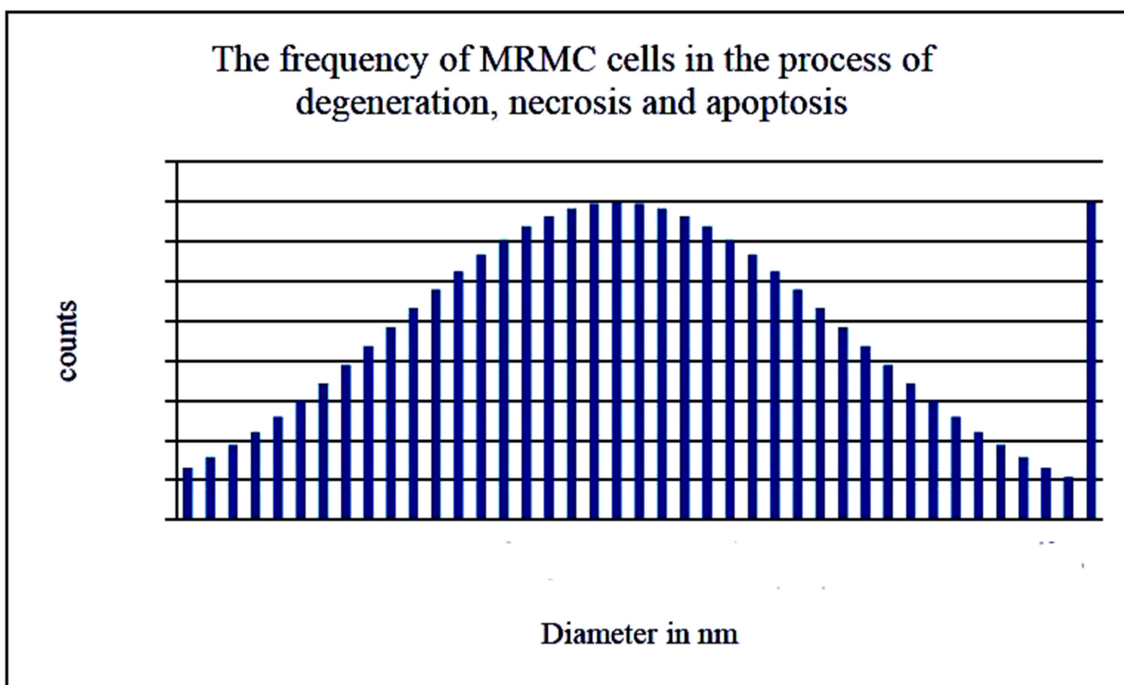


Figure 1b: Diameters ranging between 5 and 45 nm, which demonstrates that these particles are multi-dispersed, $n=400$ particles; $D_M=9,1; \sigma=0,32$.

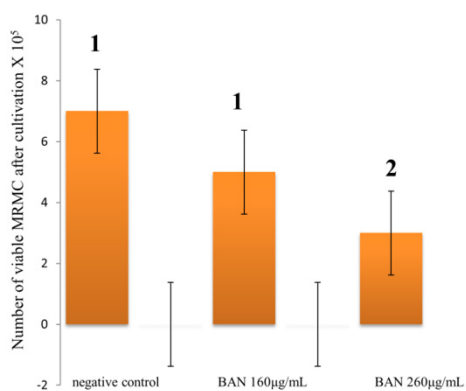


Figure 1c: Magnetic albumin polymers at the concentration 160 µg/mL allowed survival of app. 65% of MRMC, while at the concentration of 260 µg/mL, the survival rate was 60%. Different letters in the columns denote a significant difference ($p < 0.05$).

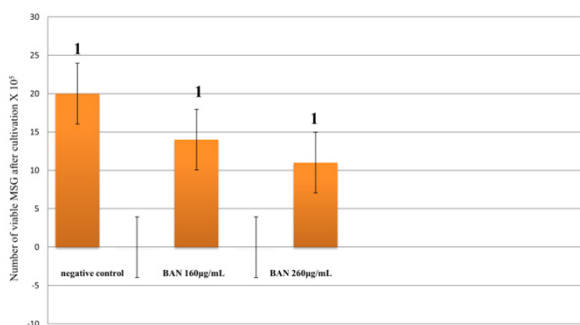


Figure 1d: For MSG, in the groups treated with 160 and 260 µg/mL, the cell survival rate was app. 55 and 70% respectively. Different numbers in the columns denote a significant difference ($p < 0.05$).

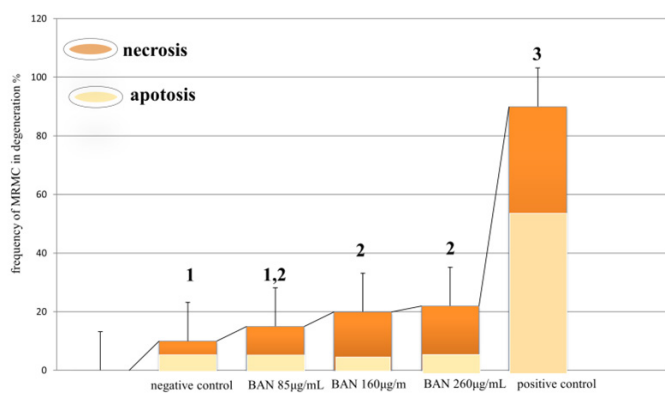


Figure 1e: Illustrates the frequency of MRMC cells in the process of degeneration, necrosis and apoptosis. Different numbers in the columns denote a significant difference ($p < 0.05$).

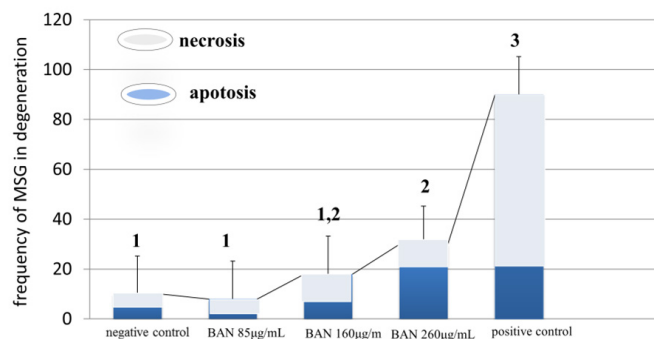


Figure 1f: In MSG the most common degeneration pathway frequent, both in the groups treated with BAN and in the untreated one was apoptosis. Different numbers in the columns denote a significant difference ($p < 0.05$).

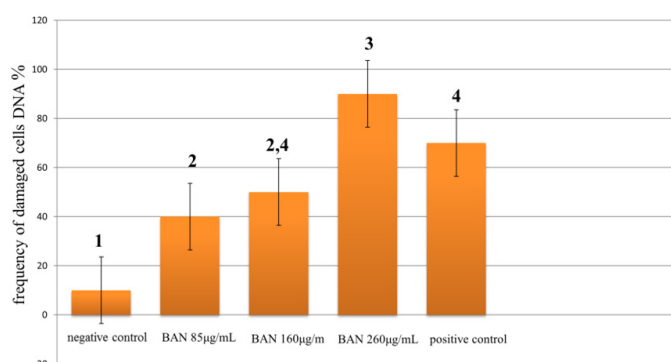


Figure 1g: Frequency of cells with DNA damage, which indicates the frequency of MRMC in each experimental group, classified as class 1, 2, 3 and 4 comets; and index of DNA damage, which reflects the intensity of DNA damage in cells. Different numbers in the columns denote a significant difference ($p < 0.05$).

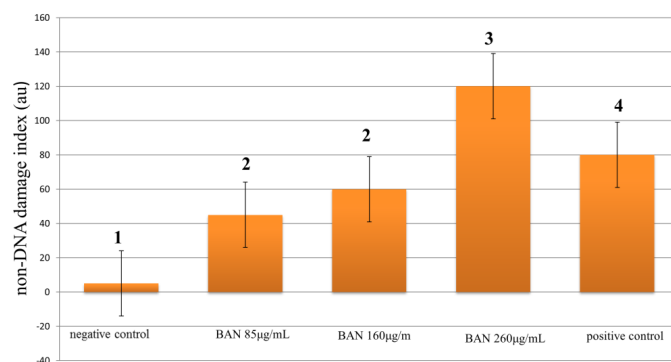


Figure 1h: Percentage of light and heavy DNA damage of MSG found in each treatment. Different numbers in the columns denote a significant difference ($p < 0.05$).

associated with cells, under the electron microscope these cells had some clusters of NPs inside, some located in the cytoplasmic projections, as can be seen in Figure 4a and 4b. Clusters of BAN were observed in greater quantity when dispersed outside the cells (Figure 4c). At TEM, MSG are characterized by having an irregular surface with protrusions, voluminous and

irregular nucleus with evident nucleoli. The cytoplasm is rich in membranous organelles such as endoplasmic reticulum, oval mitochondria and developed Golgi complex. When treated with BAN, the MSG showed no changes in ultrastructure, but had agglomerates of NPs inside (Figure 4d and 4e). The micrographs showed a greater amount of BAN agglomerates in the outside the

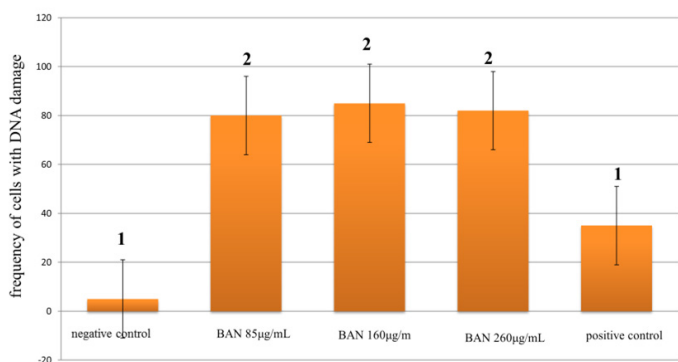


Figure 1i: The groups of MRMC treated with BAN, (85 µg/mL, 160 µg/mL and 260 µg/mL), is significantly higher than that of the control group (2.22 AU). Different letters in the columns denote a significant difference ($p < 0.05$).

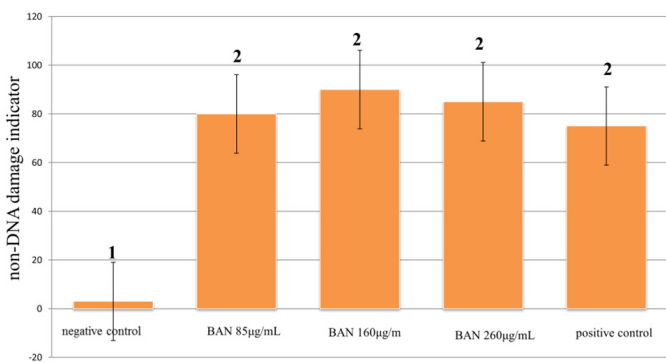


Figure 1j: Effect of BAN treatment on MRMC treated with BAN (85 µg/mL, 160 µg/mL and 260 µg/mL) on DNA damage index. Different numbers in the columns denote a significant difference ($p < 0.05$).

cells (Figure 4d). Figures 4 and 5 show TEM of MRMC and MSG subjected to different treatments: (a) negative control; (b) 85 µg/mL BAN; (c) 160 µg/mL of BAN; (d) 260 µg/mL BAN. Arrows indicate the presence of magnetic NPs clusters. Figure 5 shows TEM of MRMC subjected to different treatments: (a) negative control; (b) 85 µg/mL BAN; (c) 160 µg/mL of BAN; (d) 260 µg/mL BAN. Arrows indicate the presence of magnetic NPs clusters.

DISCUSSION

As the most abundant blood plasma protein, encapsulation of BAN in polymers constituted by this protein could confer high degree of biocompatibility to the sample^{33,34} The magnetic albumin polymers used in this study are made up of maghemite, iron oxide found in oxidized form. The fact of being in shape oxidized makes maghemite less reactive, with less potential for toxicity to cells. Maghemite NPs present lower toxicity than those of magnetite, iron oxide which is found in reduced form.³⁵ To be used in the biomedical area, in the organism, the magnetic NPs cross the endothelial barrier and accumulate specifically in target cells, without inducing damage to normal cells. NPs must therefore present characteristics that lead to its biocompatibility. Among these characteristics, the chemical nature of the NPs and their coverage. When the iron oxide NPs were free or associated with a manganese atom, induce dose-dependent toxicity and, when associated with a cobalt atom, the toxicity was higher.³⁶ Zheng, *et al.* 2019³⁷ demonstrated that NPs of the same chemical nature (magnetite), but coated with different coverage also

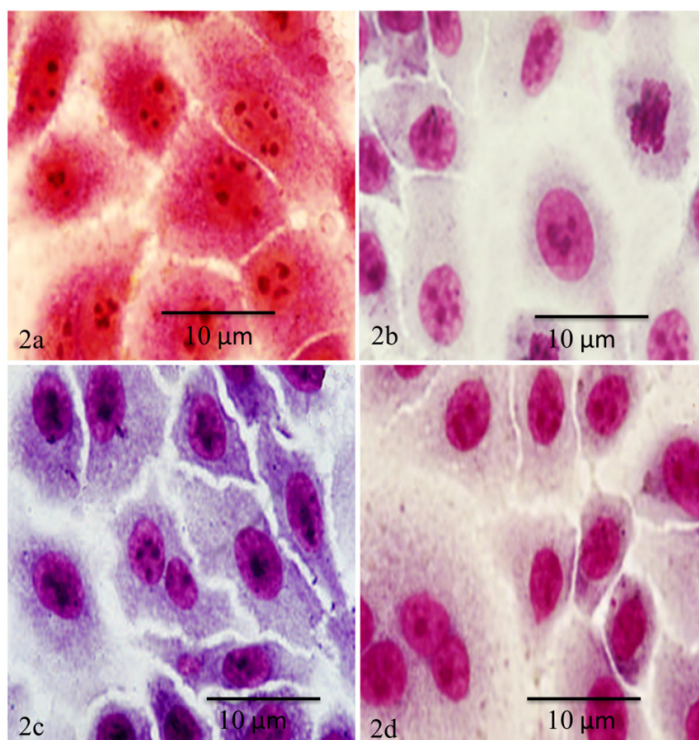


Figure 2 : Treatment with BAN, at different concentrations, did not induce changes in the morphology of these cells, as illustrated in (2a and 2b). Treatment with BAN, at different concentrations, did not induce changes in the morphology of these cells, as illustrated in (2c and 2d).

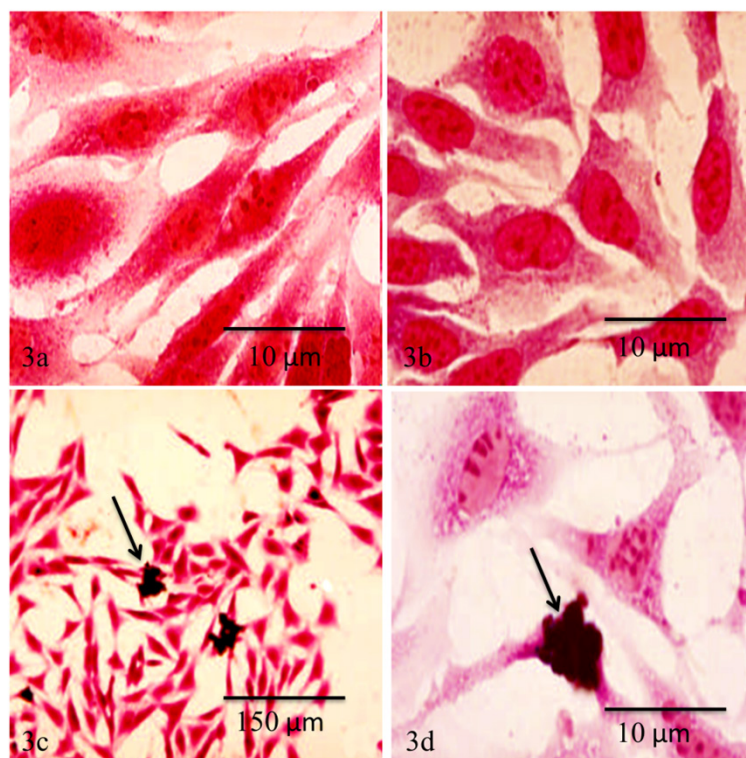


Figure 3: MSG are irregularly shaped, have long cytoplasmic processes which give a starry appearance. They have an oval, central nucleus with evident nucleoli (3a and 3b). When treated with BAN sample, the MSG did not show morphological changes (3c). Clusters of magnetic albumin polymers, apparently not internalized by cells (3d).

induced different results. However, when they were coated with albumin, they induced increase in the rate of cell proliferation. Another important factor is the size of the NPs; it is necessary that the NPs are small enough that there is no precipitation, allowing the Brownian motion acts as a dispersing agent.³⁸ In addition, the reduced size of the particles can make it difficult to recognition by the mononuclear phagocyte system. Using transmission electron microscopy, it was determined that the modal diameter of encapsulated maghemite NPs in BAN is 9.1 nm. This size is similar to that of previously tested nanoparticle samples *in vitro*,³⁹ with varying degrees of compatibility. Some *in vivo* studies show that BAN with a diameter in the 7-12 nm range has more favorable to their applications. Uniform iron oxide nanoparticles in the size range from 10 to 24 nm and polydisperse 14 nm iron oxide particles were prepared.⁴⁰

Aiming to determine the biocompatibility of polymers of magnetic albumin tests (BAN) in the present study, toxicity tests and genotoxicity were tried; in addition to evaluating the morphology and ultrastructure of MSG and MRMC cells grown in the presence of BAN. It was necessary to determine the concentration of polymers to be delivered to cells; what was done through feasibility tests performed by exclusion using the vital dye trypan blue. From the viability test with trypan blue, it was defined that the cells would be cultured in the presence of BAN at a concentration of 260 µg/mL as it was in this concentration that

BAN sample induced a significant reduction of app. 32.5 % and 61.5%, in the viability of MRMC and MSG, respectively. When the aim is to analyze *in vitro* the genotoxic effects of a compound, the concentration to be used must be defined in cytotoxicity tests. In this way, it is possible to establish the responses of a single compound in different systems or of several compounds in a single system. Therefore, in this study, with the aim of determine if the possible effects of BAN sample were dose-dependent, also if used the BAN sample in two other concentrations that corresponded to 32.5% and 61.5% the one that allowed app. the viability of 55% of the cells (260 µg/mL). This last test, however, has not been indicated to evaluate the toxicity of the NPs, because their color, both those found in the culture medium and the that are inside the cells, interferes with the reading on the spectrophotometer. In this study it was possible to verify that magnetic albumin polymers showed cytotoxic effects on MRMC and MSG. In MSG, the BAN sample induced toxicity only at the highest concentration (260 µg/mL), while in MRMC; this effect was grown in the presence of BAN. It is plausible to assume that genetic instability of MRMC is due to the fact that they are tumor-derived.⁴¹

When cell death presents all the morphological and biochemical reactions of apoptosis, but was induced by a particular compound or physical stimulus, is not a programmed process but a cellular response to changes environmental issues.⁴¹ It is known that iron, although it is an essential element for the body, when in excess can

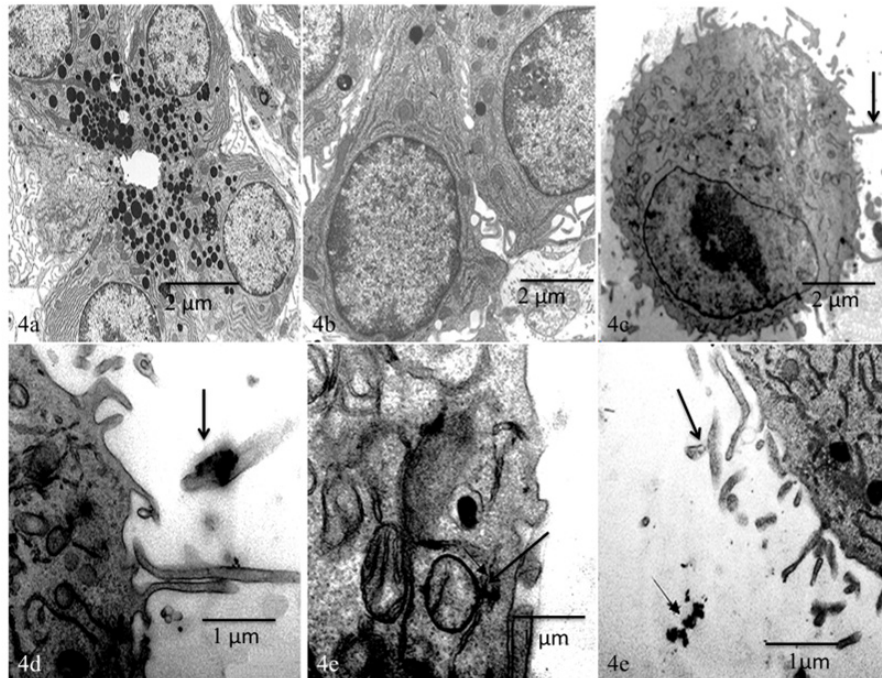


Figure 4: MSG under the electron microscope had some clusters of NPs inside, some located in the cytoplasmic projections, as can be seen in 4a and 4b. Clusters of BAN were observed in greater quantity when dispersed outside the cells (4c). At TEM, MSG is characterized by having an irregular surface with protrusions, voluminous and irregular nucleus with evident nucleoli. The cytoplasm is rich in embranous organelles such as endoplasmic reticulum, oval mitochondria and developed Golgi complex. When treated with BAN, the MSG showed no changes in ultrastructure, but had agglomerates of NPs inside (4d and 4e). The micrographs showed a greater amount of BAN agglomerates in the outside the cells (4d).

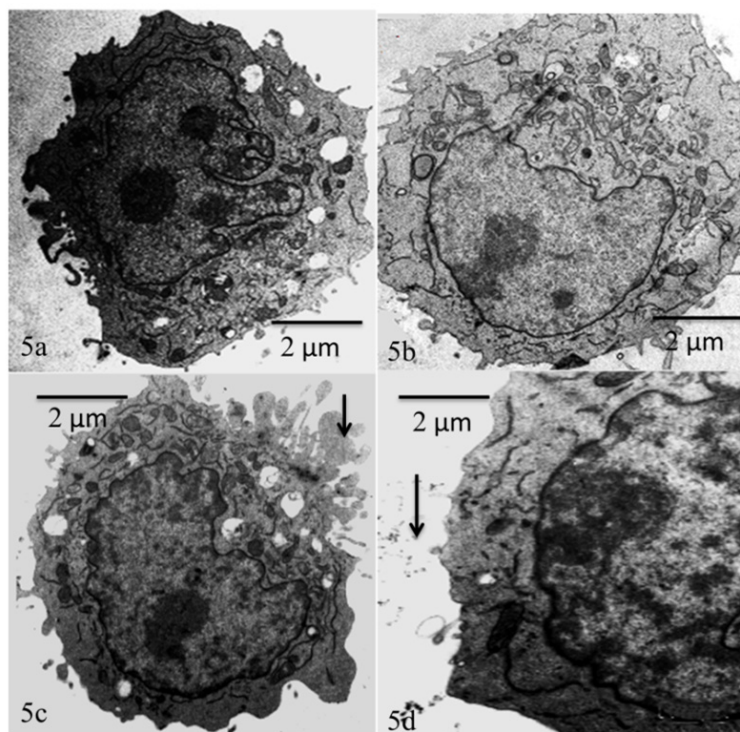


Figure 5: TEM of MRMC subjected to different treatments: (a) negative control; (b) 85 $\mu\text{g/mL}$ BAN; (c) 160 $\mu\text{g/mL}$ of BAN; (d) 260 $\mu\text{g/mL}$ BAN. Arrows indicate the presence of magnetic NPs clusters.

cause oxidative stress in cells, leading to formation of hydroxyl radicals and superoxide, causing damage to the cell membrane, proteins and DNA.⁴² In this way, the cytotoxicity and apoptosis detected in this study may have been triggered by free radicals induced by the presence of iron in BAN. The association between cytotoxicity and genotoxicity is well established, as DNA damage is considered to be an important apoptosis-inducing mechanism and necrosis.⁴³

The comet assay has been considered one of the best methods to quantify DNA damage, because of its great sensitivity, allowing measuring not only double strand breaks, but also single strand breaks, in addition to sites susceptible to alkaline attack, oxidative DNA damage, and cross-linking. In addition, genotoxicity tests such as micronucleus and cytogenetic analysis are not appropriate in cell lines with chromosomal instability, such as MRMC, since this instability would make it difficult to distinguish between intrinsic damage or caused by an experimental treatment.⁴⁴⁻⁴⁶ In MRMC and MSG, treatment with BAN sample induced an increase in frequencies of cells with DNA damage and the index of this damage in MRMC, this increase was significant for all concentrations tested, with the results with BAN sample at the highest concentration, significantly greater than those obtained with the other two concentrations. If added to the cytotoxicity data obtained by the staining assay, it can be concluded that in MRMC there may be genotoxicity without significant cytotoxicity. This conclusion can also be obtained in MSG in which BAN sample induced a similar increase in the frequencies of cells with DNA damage and on the index of this damage, while cytotoxicity significant is only verified in the highest concentration of BAN. In this work, in MRMC treated with the major concentrations, intermediate or minor of BAN sample, class 3 and 4 comets (damage intense) represented 7%, 2.3% or 2.2%, respectively, of the total cells with damage in each experimental group. In MSG these values were 1%, 0.8% and 0.1%, respectively. These values are not directly related to the highest percentages of apoptosis displayed by both cell types after BAN treatments. Various reasons could explain this fact: the continued presence of free radicals, the possibility that class 1 and 2 cells also lead cells to apoptosis, changes in repair mechanisms that make them ineffective. The morphological changes indicative of apoptosis detected in MRMC and MSG by the acridine and ethidium bromide orange staining assay, it was not confirmed under the light microscope. It is likely that cells analyzed under a light microscope represent the set of viable cells and cells in the initial phase of apoptosis, since they did not present any evident morphological alteration. Under the light microscope, no morphological alterations were found, which is interesting result regarding the use of this nanostructured material in biomedical applications. This observation was confirmed by transmission electron microscope analyzes, even in the presence of some clusters of BAN internalized in both cell types. Under the light microscope, the interiorization of BAN was not observed,

which may reflect the limitation in detecting BAN by the stains used or even death of the cells that had endocytosed BAN and subsequent loss of adhesion capacity of the same as the coverslips investigated. Cells can endocytose molecules bound to albumin that are subsequently hydrolyzed in lysosomes and released into the cytosol, where they exert their biological action.⁴⁷ Although BAN have been visualized by TEM within cells, it is important to note that these did not show absorption vesicles, a characteristic of the process of endocytosis.

CONCLUSION

This study showed that BAN presents cytotoxicity related to sample concentration and cell type; induces, as the main route of degeneration, apoptosis, which is always less than 30%; has genotoxic activity, but mostly damage of light intensity (class 1 and 2); in minor concentrations, may present genotoxic activity and do not have corresponding cytotoxic; showed no alterations in the morphology or ultrastructure of both cells; had its BAN internalized by some cells. In studies of nanoparticle-cell interactions carried out *in vitro*, it is plausible expect more severe effects than those performed *in vivo*, since living organisms have a series of mechanisms to restore the homeostatic balance, which are absent in cell cultures and therefore describe a situation of acute cytotoxicity. Based on the results obtained in this study, it is possible to conclude that, under the experimental conditions using the BAN sample: Different cellular patterns can be observed and classified: Living cells have a uniform green nucleus; Cells in early stages of apoptosis still have their membranes intact and, therefore, they have a green nucleus, but not uniformly colored. Chromatin condensation, DNA cleavage and/or nuclear fragmentation occur; Cells in late stages of apoptosis show chromatin condensation and orange areas in the nucleus. Because in the final stages of the process already lost membrane integrity and BE predominates over AA. Apoptotic cells may still have apoptotic bodies; Necrotic cells have lost membrane integrity and therefore present uniform orange core. While the results obtained in this article point to the biocompatibility of the sample of magnetic albumin polymers, other studies should be carried out in order to establish an *in vivo* experimental model for better clarify the biocompatibility of magnetic albumin polymers.

ACKNOWLEDGEMENT

The author acknowledges the Deanship of Scientific Research; the Ministry of Higher Education at Imam Abdulrahman bin Faisal University for supporting this study.

ETHICAL STATEMENT

Ethical clearance for this study was obtained from the Imam Abdulrahman bin Faisal University ethics committee. The author of this study respected the value of the experimented mice. He respected that mice are sentient creatures with the capacity to

feel pain. The treatment of animals, including the use of animals in research, is an expression of the researcher's attitudes and influences him as a moral actor. The minimal number of mice as possible was used in this experiment.

CONFLICT OF INTEREST

The authors declare that there is no conflict of interest.

ABBREVIATIONS

BAN: Bovine Albumin Nanoparticles; **NPs:** Nanoparticles; **MSG:** Mouse Submandibular Salivary Gland; **MRMC:** Mouse Renal Mesangial Cells.

SUMMARY

The study reveals that magnetic albumin (BAN) exhibits cytotoxicity based on sample concentration and cell type, causing apoptosis and genotoxic activity. It also shows no alterations in cell morphology or ultrastructure and may be internalized by some cells. *In vitro* studies may have more severe effects than *in vivo* studies, as living organisms have mechanisms to restore homeostatic balance. Different cellular patterns can be observed under experimental conditions using BAN samples, including living cells with a uniform green nucleus, early apoptosis cells with chromatin condensation, late apoptosis cells with orange areas, and apoptotic cells with a uniform orange core.

REFERENCES

- Khan I, Saeed K, Khan I. Nanoparticles: properties, applications and toxicities. Arab J Chem. 2019;12(7):908-31. doi: 10.1016/j.arabj.2017.05.011.
- Szczylgiewska P, Feliczyk-Guzik A, Nowak I. Nanotechnology—general aspects: A chemical reduction approach to the synthesis of nanoparticles. Molecules. 2023;28(13):4932. doi: 10.3390/molecules28134932, PMID 37446593.
- McNamara K, Tofail SAM. Nanoparticles in biomedical applications. Adv Phys X. 2017;2(1):54-88. doi: 10.1080/23746149.2016.1254570.
- Chen BA, Jin N, Wang J, Ding J, Gao C, Cheng J, et al. The effect of magnetic nanoparticles of Fe₃O₄ on immune function in normal ICR mice. Int J Nanomedicine. 2010;5:593-9. doi: 10.2147/ijn.s12162, PMID 20856834.
- Xuan MV, Dang PN, Quang LD, Minh HN, Duc TC, Thanh TB. Highly sensitive modified giant magnetometer resistance measurement system for the determination of superparamagnetic nanoparticles in continuous flow with application for the separation of biomarkers. Instrum Sci Technol. 2022:1-18.
- Al-Musawi S, Ibraheem S, Abdul Mahdi S, Albukhary S, Haider AJ, Kadhim AA, et al. Smart nanoformulation based on polymeric magnetic nanoparticles and vincristine drug: A novel therapy for apoptotic gene expression in tumors. Life (Basel). 2021;11(1):71. doi: 10.3390/life11010071, PMID 33478036.
- Yildiz I. Applications of magnetic nanoparticles in biomedical separation and purification. Nanotechnol Rev. 2016;5(3):331-40. doi: 10.1515/ntrev-2015-0012.
- Alvieri F, Mamani JB, Nucci MP, Oliveira FA, Filgueiras IS, Rego GNA, et al. Methods of granulocyte isolation from human blood and labeling with multimodal superparamagnetic iron oxide nanoparticles. Molecules. 2020;25(4). doi: 10.3390/molecules25040765, PMID 32053865.
- Papadimitriou CA, Roots A, Koenigsmann M, Koenigsmann M, Mücke C, Oelmann E, et al. Immunomagnetic selection of CD34+ cells from fresh peripheral blood mononuclear cell preparations using two different separation techniques. J Hematother. 1995;4(6):539-44. doi: 10.1089/scd.1.1995.4.539, PMID 8846014.
- Patra JK, Das G, Fraceto LF, Campos EVR, Rodriguez-Torres MDP, Acosta-Torres LS, et al. Nano based drug delivery systems: recent developments and future prospects. J Nanobiotechnology. 2018;16(1):71. doi: 10.1186/s12951-018-0392-8, PMID 30231877.
- Caster JM, Patel AN, Zhang T, Wang A. Investigational nanomedicines in 2016: a review of nanotherapeutics currently undergoing clinical trials. Wiley Interdiscip Rev Nanomed Nanobiotechnol. 2017;9(1):e1416. doi: 10.1002/wnan.1416, PMID 27312983.

- Hale GR, Teplitsky S, Truong H, Gold SA, Bloom JB, Agarwal PK. Lymph node imaging in testicular cancer. Transl Androl Urol;5: 2018;7:864-874. doi: 10.21037/tau.2018.07.18.
- Sharifianjazi F, Jafari Rad AJ, Bakhtiari A, Niazvand F, Esmailkhanian A, Bazli L, et al. Biosensors and nanotechnology for cancer diagnosis (lung and bronchus, breast, prostate, and colon): a systematic review. Biomed Mater. 2021;17(1). doi: 10.1088/1748-605X/ac41fd, PMID 34891145.
- Cui D, Zhang C, Liu B, Shu Y, Du T, Shu D, et al. Regression of gastric cancer by systemic injection of RNA nanoparticles carrying both ligand and siRNA. Sci Rep. 2015;5(1):10726. doi: 10.1038/srep10726, PMID 26137913.
- Liu JF, Jang B, Issadore D, Tsourkas A. Use of magnetic fields and nanoparticles to trigger drug release and improve tumor targeting. Wiley Interdiscip Rev Nanomed Nanobiotechnol. 2019;11(6):e1571. doi: 10.1002/wnan.1571, PMID 31241251.
- Heidari Majd MM, Asgari D, Barar J, Valizadeh H, Kafil V, Coukos G, et al. Specific targeting of cancer cells by multifunctional mitoxantrone-conjugated magnetic nanoparticles. J Drug Target. 2013;21(4):328-40. doi: 10.3109/1061186X.2012.750325, PMID 23293842.
- Giustini AJ, Petryk AA, Cassim SM, Tate JA, Baker I, Hoopes PJ. Magnetic nanoparticle hyperthermia in cancer treatment. Nano Life. 2010;1(1n02). doi: 10.1142/S1793984410000067, PMID 24348868.
- Huynh NT, Roger E, Lautram N, Benoît JP, Passirani C. The rise and rise of stealth nanocarriers for cancer therapy: passive versus active targeting. Nanomedicine (Lond). 2010;5(9):1415-33. doi: 10.2217/nm.10.113, PMID 21128723.
- Spiotto M, Fu YX, Weichselbaum RR. The intersection of radiotherapy and immunotherapy: mechanisms and clinical implications. Sci Immunol. 2016;1(3). doi: 10.1126/sciimmunol.aag1266, PMID 28018989.
- Arany S, Benoit DS, Dewhurst S, Ovitt CE. Nanoparticle-mediated gene silencing confers radioprotection to salivary glands *in vivo*. Mol Ther. 2013;21(6):1182-94. doi: 10.1038/mt.2013.42, PMID 23511246.
- Galaly SR, Abdella EM, Mohammed HM, khadrawy SM. Effects of royal jelly on genotoxicity and nephrotoxicity induced by valproic acid in albino mice. Beni Suef Univ J Basic Appl Sci. 2014;3(1):1-15. doi: 10.1016/j.bjbas.2014.02.001.
- Wong CY, Cheong SK, Mok PL, Leong CF. Differentiation of human mesenchymal stem cells into mesangial cells in post-glomerular injury murine model. Pathology. 2008;40(1):52-7. doi: 10.1080/00313020701716367, PMID 18038316.
- Noll BD, Grdzlishvili A, Brennan MT, Mougeot FB, Mougeot JC. Immortalization of salivary gland epithelial cells of xerostomic patients: establishment and characterization of novel cell lines. J Clin Med. 2020;9(12). doi: 10.3390/jcm9123820, PMID 33255850.
- Yu H, Cui S, Mei Y, Li Q, Wu L, Duan S, et al. Mesangial cells exhibit features of antigen-presenting cells and activate CD4+ T cell responses. J Immunol Res. 2019; 2019:2121849. doi: 10.1155/2019/2121849, PMID 31317046.
- Nosrati H, Sefidi N, Sharafi A, Danafar H, Kheiri Manjili HK. Bovine serum albumin (BSA) coated iron oxide magnetic nanoparticles as biocompatible carriers for curcumin-anticancer drug. Bioorg Chem. 2018;76:501-9. doi: 10.1016/j.bioorg.2017.12.033, PMID 29310081.
- Menè P, Stoppacciaro A. Isolation and propagation of glomerular mesangial cells. Methods Mol Biol. 2009;466:3-17. doi: 10.1007/978-1-59745-352-3_1, PMID 19148614.
- Alsamamra H, Hawwarin I, Abu Sharkh S, Abuteir M. Study the interaction between gold nanoparticles and bovine serum albumin: spectroscopic approach. J Bioanal Biomed; 2018. p. hal-04033898. version 1. doi: 10.4172/1948-593x.1000203.
- García-Rodríguez MdC, Carvente-Juárez MM, Altamirano-Lozano MA. Antigenotoxic and apoptotic activity of green tea polyphenol extracts on hexavalent chromium-induced DNA damage in peripheral blood of CD-1 mice: analysis with differential acridine orange/ethidium bromide staining. Oxid Med Cell Longev. 2013; 2013:486419. doi: 10.1155/2013/486419, PMID 24363823.
- Cortés-Gutiérrez El, Dávila-Rodríguez MI, Fernández JL, López-Fernández C, Gosálbez A, Gosálvez J. New application of the comet assay: chromosome--comet assay. J Histochem Cytochem. 2011;59(7):655-60. doi: 10.1369/0022155411410884, PMID 21540337.
- Yu Z, Yu M, Zhang Z, Hong G, Xiong Q. Bovine serum albumin nanoparticles as controlled release carrier for local drug delivery to the inner ear. Nanoscale Res Lett. 2014;9(1):343. doi: 10.1186/1556-276X-9-343, PMID 25114637.
- Tran SL, Puhar A, Ngo-Camus M, Ramarao N. Trypan blue dye enters viable cells incubated with the pore-forming toxin HlyII of *Bacillus cereus*. PLOS ONE. 2011;6(9):e22876. doi: 10.1371/journal.pone.0022876, PMID 21909398.
- Ammerman NC, Beier-Sexton M, Azad AF. Growth and maintenance of Vero cell lines. Curr Protoc Microbiol. 2008;Appendix(4):Appendix 4E. doi: 10.1002/9780471792259.mca04es11, PMID 19016439. Appendix 4.
- Topalá T, Bodoki A, Oprean L, Oprean R. Bovine serum albumin interactions with metal complexes. Clujul Med. 2014;87(4):215-9. doi: 10.15386/cjmed-357, PMID 26528027.
- Raoufina R, Mota A, Keyhanvar N, Safari F, Shamekhi S, Abdolalazadeh J. Overview of albumin and its purification methods. Adv Pharm Bull. 2016;6(4):495-507. doi: 10.15171/apb.2016.063, PMID 28101456.
- Singh N, Jenkins GJS, Asadi R, Doak SH. Potential toxicity of superparamagnetic iron oxide nanoparticles (SPION). Nano Rev. 2010;1(1):5358. doi: 10.3402/nano.v1i0.5358, PMID 22110864.

36. Kim HR, Kim MJ, Lee SY, Oh SM, Chung KH. Genotoxic effects of silver nanoparticles stimulated by oxidative stress in human normal bronchial epithelial (BEAS-2B) cells. *Mutat Res.* 2011;726(2):129-35. doi: 10.1016/j.mrgentox.2011.08.008, PMID 21945414.
37. Zheng F, Luo Z, Zheng C, Li J, Zeng J, Yang H, *et al.* Comparison of the neurotoxicity associated with cobalt nanoparticles and cobalt chloride in Wistar rats. *Toxicol Appl Pharmacol.* 2019;369:90-9. doi: 10.1016/j.taap.2019.03.003, PMID 30849457.
38. Paul G, Sarkar S, Pal T, Das PK, Manna I. Concentration and size dependence of nano-silver dispersed water based nanofluids. *J Colloid Interface Sci.* 2012;371(1):20-7. doi: 10.1016/j.jcis.2011.11.057, PMID 22284450.
39. Sutradhar S, Das S, Roychowdhury A, Das D, Chakrabarti PK. Magnetic property, Mössbauer spectroscopy and microwave reflection loss of maghemite nanoparticles (γ -Fe₂O₃) encapsulated in carbon nanotubes, *Materials Science and Engineering: B*, 2015, 196: 44-52. <https://doi.org/10.1016/j.mseb.2015.02.008>
40. Patsula V, Moskvina M, Dutz S, Horák D. Size-dependent magnetic properties of iron oxide nanoparticles. *J Phys Chem Solids.* 2016;88:24-30. doi: 10.1016/j.jpcs.2015.09.008.
41. Doi T, Vlassara H, Kirstein M, Striker LJ. Receptor-specific increase in extracellular matrix production in mouse mesangial cells by advanced glycosylation end products is mediated via platelet-derived growth factor. *PNAS.* 1992;89(7):2873-7. doi: 10.1073/pnas.89.7.2873.
42. Miller MA, Zachary JF. Mechanisms and morphology of cellular injury, adaptation, and death. *Pathologic Basis Vet Dis.* 2017;2-43.e19. doi: 10.1016/B978-0-323-35775-3.00001-1.
43. Pizzino G, Irrera N, Cucinotta M, Pallio G, Mannino F, Arcoraci V, *et al.* Oxidative stress: harms and benefits for human health. *Oxid Med Cell Longev.* 2017; 2017:8416763. doi: 10.1155/2017/8416763, PMID 28819546.
44. Zhang L, Wang X, Zou J, Liu Y, Wang J. DMSA-coated iron oxide nanoparticles greatly affect the expression of genes coding cysteine-rich proteins by their DMSA coating. *Chem Res Toxicol.* 2015;28(10):1961-74. doi: 10.1021/acs.chemrestox.5b00161, PMID 26378955.
45. Schmeiser HH, Muehlbauer KR, Mier W, Baranski AC, Neels O, Dimitrakopoulou-Strauss A, *et al.* DNA damage in human whole blood caused by radiopharmaceuticals evaluated by the comet assay. *Mutagenesis.* 2019;34(3):239-44. doi: 10.1093/mutage/gez007, PMID 31107537.
46. Collins AR. The comet assay for DNA damage and repair: principles, applications, and limitations. *Mol Biotechnol.* 2004;26(3):249-61. doi: 10.1385/MB:26:3:249, PMID 15004294.
47. O'Brien K, Breyne K, Ughetto S, Laurent LC, Breakefield XO. RNA delivery by extracellular vesicles in mammalian cells and its applications. *Nat Rev Mol Cell Biol.* 2020;21(10):585-606. doi: 10.1038/s41580-020-0251-y, PMID 32457507.

Cite this article: Qurashi NA. Study of the Effect of Magnetic Serum Albumin Nanoparticles on Cultured Mice Renal Mesangial Cells and Submandibular Cells Using Different Biological Assays. *Indian J of Pharmaceutical Education and Research.* 2024;58(3s):s815-s827.